LETTER TO THE EDITOR

Treatment of autosomal recessive hearing loss via in vivo CRISPR/Cas9-mediated optimized homology-directed repair in mice

Cell Research (2022) 32:699–702; https://doi.org/10.1038/s41422-022-00624-y

Dear Editor,

Hearing loss is the most common sensory disorder in the world. Among cases of non-syndromic hearing loss, which account for 70% of all cases of genetic hearing loss, around 80% of cases arise from autosomal recessive loss-of-function mutations that require repair, rather than disruption, of the mutant allele.[1] CRISPR/Cas9-mediated homology-directed repair (HDR)-based therapies have the potential to cure many genetic diseases because this class of therapeutics can achieve arbitrary base changes as well as the insertion or deletion of DNA fragments.[2] However, HDR is considered to be largely restricted to dividing cells and is generally inefficient in animal tissues in vivo.[3] CRISPR/Cas9-mediated HDR has been successfully used to efficiently correct the *Cdh23*^{ahl} allele in C57BL/6NTac zygotes and to rescue the associated auditory phenotype.[4] However, there have been no reports of applying this strategy at the postnatal stage (i.e., in vivo) to achieve hearing preservation in animal models of hereditary hearing loss. An efficient HDR strategy in nondividing mammalian cells (including cochlear hair cells) holds promise for developing treatments for recessive hearing loss. We previously devised a new homology-mediated end joining (HMEJ)-based strategy using CRISPR/Cas9-mediated cleavage of the transgene donor vector, which contains guide RNA target sites and ~800 bp of homology arms, and cleavage of the targeted site in the genome[5] (Supplementary information, Fig. S1). This approach, which is an optimized version of HDR, achieved transgene integration in mouse and monkey embryos, as well as in hepatocytes and neurons in vivo, with an efficiency much greater than homologous recombination- and nonhomologous end joining-based strategies.[5]

In this work, homozygous *Klhl18*^{lowf} mice were used as a model of recessive hereditary hearing loss, as reported by Ingham et al.[6] *Klhl18*^{lowf} mutant allele contains a missense (p.V55F) point mutation (Chr9:110455454 C>A) of *Klhl18* that cannot be corrected using current base-editing strategies. The mutation in *Klhl18* leads to the dysfunction of inner hair cells (IHCs), which results in abnormal auditory brainstem response (ABR) but normal distortion product otoacoustic emission (DPOAE) thresholds.[6] Homozygous *Klhl18*^{lowf} mutant mice showed abnormally tapering of the tips of IHC stereocilia, especially in the apical and middle turns of the cochlea. However, hair cell degeneration was not observed in the homozygous mutants.[6]

Firstly, via testing three single-guide RNAs (sgRNAs), we managed to identify a highly efficient sgRNA that specifically targets the *Klhl18*^{lowf} site in primary neonatal fibroblasts derived from homozygous *Klhl18*^{lowf} mice (Fig. 1a; Supplementary information, Fig. S2a and Data S1); the editing efficiency of each SaCas9-KKH–sgRNA composite from high to low showed an order of sgRNA2 > sgRNA3 > sgRNA1 (Fig. 1b; Supplementary information, Fig. S2b and Table S1). It has been reported that the efficiency of homologous recombination has an inverse correlation with the distance between the point mutation site and the cleavage position.[7] Therefore, sgRNA2 was chosen for the subsequent experiments.

Because sgRNA2 does not cover the *Klhl18*^{lowf} mutation site, we introduced a synonymous mutation site on the donor to prevent potential sgRNA2-induced cleavage of the template or secondary cleavage of the corrected sequence (Fig. 1a). By constructing an NIH3T3 cell line expressing donor template via a lentiviral system, we confirmed that sgRNA2 produced significant editing of the endogenous locus without editing the donor template (Supplementary information, Fig. S3a, b, and Table S1).

We next constructed the HMEJ-based agents that consist of two plasmids (Supplementary information, Fig. S4a) for in vitro examination of the editing efficiency. By fluorescence-based cell sorting, we found a 17.8-fold increase of indel efficiency in the sorted cells compared to the unsorted sample (from 1.2% to 21.3%) (Fig. 1b, c; Supplementary information, Table S1). We also observed a distinct corrected population of fibroblasts compared to the mock-transfected controls (Fig. 1c; Supplementary information, Fig. S4b). No obvious indel mutations for the off-target sites were detected in homozygous *Klhl18*^{lowf} fibroblasts transfected with SaCas9-KKH + sgRNA2, indicating the high fidelity of this CRISPR/Cas9 system (Fig. 1d; Supplementary information, Table S2).

Given the high transduction efficiency of AAV9 and AAV-PHP.eB in IHCs,[8] we used these two AAVs to package the CRISPR/Cas9 knock-in system for delivery into the inner ear (Fig. 1e). The AAV–sgRNA–donor transduced more than 93% of the IHCs on average 10 weeks after injection (Fig. 1f; Supplementary information, Fig. S5). For the whole cochlear tissue collected from the injected ears of homozygous mutants, the in vivo correction efficiency was increased by 3.2-fold at 10 weeks of age compared to P14 (from 0.10% to 0.32%), while no obvious indels or gene corrections were observed in the samples from the non-injected ears (Fig. 1g, h; Supplementary information, Fig. S6 and Table S1). These results indicate that the correction efficiency was increased with increased editing time. It has been reported that hair cells in the dissected organ of Corti make up only about 1.5% of the total cells used for deep sequencing,[9] which indicates the actual correction efficiency was underrepresented. We also assessed off-targeting of the therapeutic agents in vivo by whole-genome sequencing, and no obvious indels or SNPs were detected (Supplementary information, Fig. S7 and Table S3).

Klhl18 has Kelch-repeat domains that interact with actin.[10] Deficiency in Klhl18 may therefore result in a range of cellular

Received: 19 May 2021 Accepted: 13 January 2022
Published online: 23 February 2022

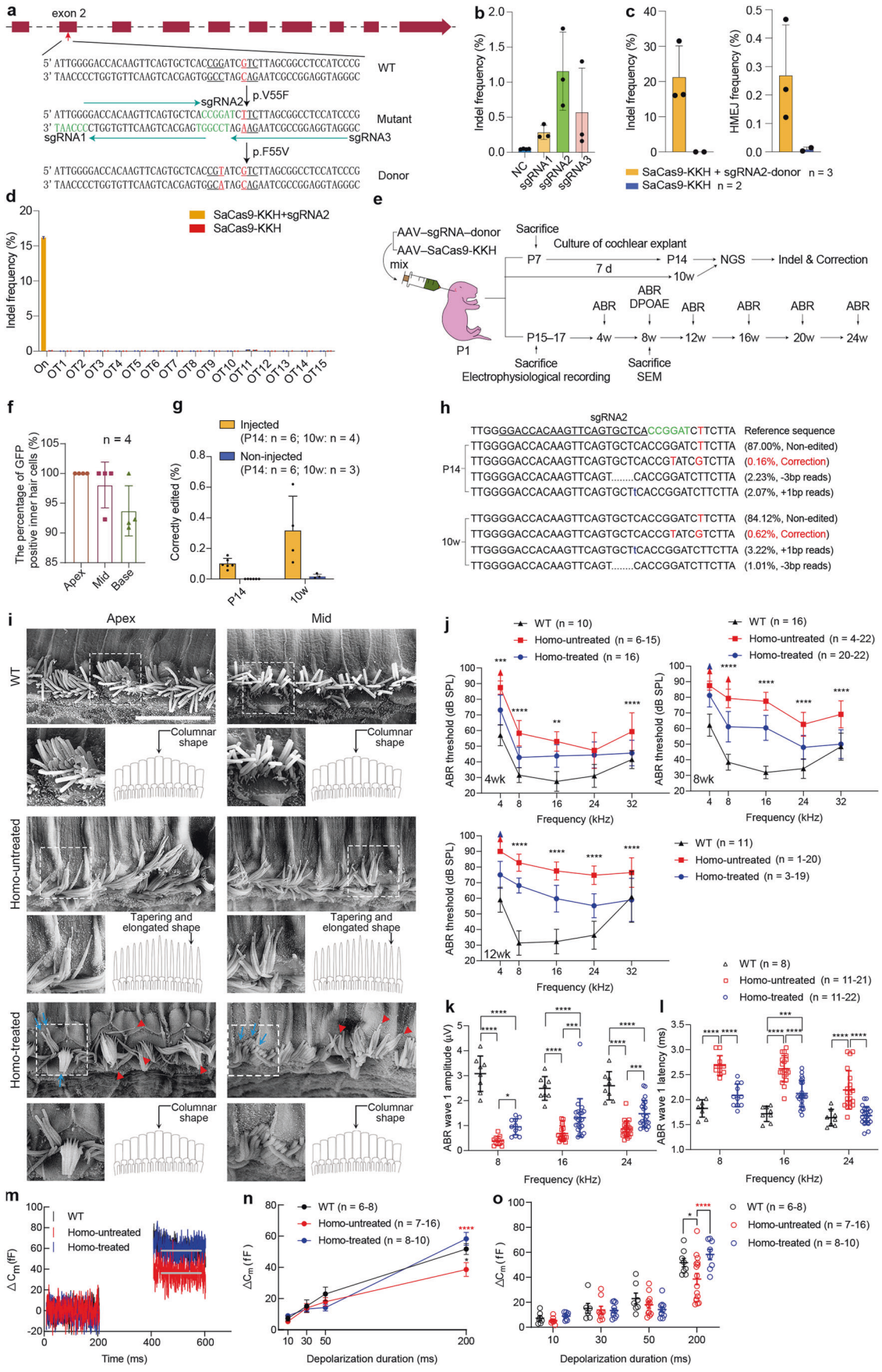
a
exon 2
WT
sgRNA2
p.V55F
Mutant
sgRNA1
sgRNA3
p.F55V
Donor
b
Indel frequency (%)
NC
sgRNA1
sgRNA2
sgRNA3
c
Indel frequency (%)
HMEJ frequency (%)
SaCas9-KKH + sgRNA2-donor n = 3
SaCas9-KKH n = 2
d
SaCas9-KKH+sgRNA2
SaCas9-KKH
Indel frequency (%)
On
OT1
OT2
OT3
OT4
OT5
OT6
OT7
OT8
OT9
OT10
OT11
OT12
OT13
OT14
OT15
e
AAV–sgRNA–donor
AAV–SaCas9-KKH
mix
P1
Sacrifice
Culture of cochlear explant
P7
P14
NGS
Indel & Correction
7 d
10w
ABR
DPOAE
P15–17
4w
8w
12w
16w
20w
24w
Sacrifice
Electrophysiological recording
Sacrifice
SEM
f
n = 4
The percentage of GFP positive inner hair cells (%)
Apex
Mid
Base
g
Injected
(P14: n = 6; 10w: n = 4)
Non-injected
(P14: n = 6; 10w: n = 3)
Correctly edited (%)
P14
10w
h
sgRNA2
Reference sequence
P14
(87.00%, Non-edited)
(0.16%, Correction)
(2.23%, -3bp reads)
(2.07%, +1bp reads)
10w
(84.12%, Non-edited)
(0.62%, Correction)
(3.22%, +1bp reads)
(1.01%, -3bp reads)
i
Apex
Mid
WT
Homo-untreated
Homo-treated
Columnar shape
Tapering and elongated shape
j
WT (n = 10)
Homo-untreated (n = 6-15)
Homo-treated (n = 16)
WT (n = 16)
Homo-untreated (n = 4-22)
Homo-treated (n = 20-22)
ABR threshold (dB SPL)
4wk
8wk
12wk
Frequency (kHz)
WT (n = 11)
Homo-untreated (n = 1-20)
Homo-treated (n = 3-19)
k
WT (n = 8)
Homo-untreated (n = 11-21)
Homo-treated (n = 11-22)
ABR wave 1 amplitude (μV)
l
ABR wave 1 latency (ms)
Frequency (kHz)
m
WT
Homo-untreated
Homo-treated
ΔCm (fF)
Time (ms)
n
WT (n = 6-8)
Homo-untreated (n = 7-16)
Homo-treated (n = 8-10)
ΔCm (fF)
Depolarization duration (ms)
o
WT (n = 6-8)
Homo-untreated (n = 7-16)
Homo-treated (n = 8-10)
ΔCm (fF)
Depolarization duration (ms)

Fig. 1 The HMEJ-based system corrects the *Klhl18*^{lowf} point mutation, restores IHC stereocilia morphology and exocytosis, and improves hearing function in homozygous *Klhl18*^{lowf} mice. a Design of the sgRNAs and donor based on SaCas9-KKH. The mutation site is highlighted in red. Nucleotides of the PAM sites are marked in green. **b** Indel frequencies of the three sgRNAs in *Klhl18*$^{lowf/lowf}$ fibroblasts without GFP-sorting. $n = 3$ for each gRNA; $n = 4$ for negative control (NC). **c** The percentages of indels and correctly edited reads in *Klhl18*$^{lowf/lowf}$ fibroblasts after HMEJ-based gene editing and GFP-sorting. **d** Indel frequencies at the *Klhl18*^{lowf} mutation locus and each of the off-target loci detected in *Klhl18*$^{lowf/lowf}$ fibroblasts. On, on-target; OT, off-target. $n = 2$. **e** Schematic of the dual-AAV system and the experimental overview of the in vivo studies. **f** Transduction efficiencies in IHCs. With a viral dose of 1.6×10^{10} virus genomes, AAV–sgRNA–donor transduced 100.0 ± 0.0%, 98.1 ± 3.9%, and 93.7 ± 4.2% IHCs in the apical, middle, and basal turns of the cochlea, respectively. **g** The percentages of correctly edited reads from the injected and non-injected *Klhl18*$^{lowf/lowf}$ ears at P14 and 10 weeks of age respectively. Dots represent individual values, and bars represent means ± SD in **b**–**d**, **f** and **g**. **h** Deep-sequencing results for the injected cochleae with the highest correction frequency (marked by red) at P14 and 10 weeks of age, respectively. The correctly edited allele and the top 2 indel mutation types are shown along with the frequency for each mutation type. **i** Representative SEM images of the apical and middle turns of the cochleae harvested at 8 weeks of age and corresponding IHC schematic diagrams showing the morphology of the IHC stereocilia for WT (upper), non-injected homozygous (Homo-untreated; middle), and injected homozygous *Klhl18*^{lowf} (Homo-treated; lower) ears. The images from white dotted boxes are magnified for better presentation and identification. Blue arrows indicate stereocilia with columnar shape in rescued IHCs, while red arrowheads indicate tapering and elongated stereocilia in abnormal IHCs. The scale bars are 10 μm. **j** Means ± SD of the ABR thresholds for WT, non-injected, and injected homozygous *Klhl18*^{lowf} ears tested at 4, 8, and 12 weeks of age. The asterisks indicate the comparison of the ABR thresholds between the non-injected and injected ears. Arrows indicate that there were cases of no ABR response at 90 dB for the corresponding frequencies and ears. **k**, **l** Peak amplitudes (**k**) and latencies (**l**) of ABR wave 1 evoked by 90 dB stimuli in WT, injected, and non-injected homozygous *Klhl18*^{lowf} ears around 8 weeks of age. **m** Representative ΔC_m in IHCs from WT, non-injected, and injected homozygous *Klhl18*^{lowf} cochleae in response to a 200 ms depolarization pulse at maximum I_{Ca} potentials. **n** Average ΔC_m from IHCs of WT, non-injected, and injected homozygous *Klhl18*^{lowf} cochleae with voltage steps of 10–200 ms. **o** The scatter plot of **n**. The black asterisk (*) represents the result of statistical analysis comparing the ΔC_m of IHCs between WT and non-injected homozygous *Klhl18*^{lowf} cochleae. The red asterisks (****) represent the comparison of ΔC_m between injected and non-injected groups. In **j**–**l**, **n** and **o**, statistical tests were two-way ANOVAs with Bonferroni correction. *$P < 0.05$, **$P < 0.01$, ***$P < 0.001$, ****$P < 0.0001$.

problems in actin-rich cells such as IHCs and affect the actin core of stereocilia leading to a tapering phenotype of IHCs.[6] By scanning electron microscopy (SEM) (Fig. 1i), we found clear rescue of IHC stereocilia morphology 8 weeks after injection of dual AAV system based on the observation method reported by Ingham et al.[6] The IHCs in the untreated homozygous mutants showed frequent tapering of the tallest stereocilia towards their tips. The stereocilia in the mutants were also more elongated and thinner than those in wild type (WT) mice. With injection of the dual-AAV system, some IHCs in the homozygous *Klhl18*^{lowf} cochlea had normal stereocilia morphology (resembling the WT IHCs), while some neighboring IHCs showed abnormal stereocilia shape (Fig. 1i). The criteria for estimating recovery are that most of the stereocilia in the tallest row within a single bundle have a normal columnar shape and that they are shorter compared to those of the untreated mutants. In the treated cochleae of homozygous mutants, we observed that approximately 16.5 ± 9.2% and 16.9 ± 8.2% of the IHCs in the apical and middle turns respectively (from five independent samples) exhibited normal or near normal stereocilia bundles.

Klhl18^{lowf} heterozygotes showed no obvious differences in ABR thresholds across all tested frequencies compared with their WT littermates (Supplementary information, Fig. S8a–e), which is consistent with Ingham's report.[6] The untreated homozygous mutants showed progressive hearing loss with onset before 4 weeks of age. After injection of the dual-AAV system, we observed significant restoration of hearing function in treated ears compared with untreated ears at most frequencies at ages of 4–24 weeks (Fig. 1j; Supplementary information, Figs. S9, S10a–c, and Table S4). With the progression of hearing dysfunction, the proportion of cases without detectable ABR thresholds at 90 dB SPL was markedly increased at all the tested frequencies in untreated homozygous mutants, while the treated homozygous mice showed evoked ABRs at 90 dB SPL at the frequencies of 8, 16, and 24 kHz during the observation period up to 24 weeks of age. Moreover, the dual-AAV system significantly improved ABR wave 1 amplitude and latency at 4 weeks (Supplementary information, Fig. S11) and 8 weeks of age (Fig. 1k, l). The injection of AAV–SaCas9-KKH alone could not prevent hearing loss in *Klhl18*^{lowf} homozygotes, which suggests that the hearing preservation requires the dual AAVs (Supplementary information, Fig. S12). Homozygous *Klhl18*^{lowf} mice showed normal DPOAE responses at the age of 8 weeks, which was consistent with the phenotype of unaffected outer hair cells (OHCs), and the injection of AAVs did not affect the function of OHCs (Supplementary information, Fig. S13).

Ca^{2+}-triggered exocytosis of IHC synaptic vesicles was measured as plasma membrane capacitance increments (ΔC_m) after short and long depolarization pulses (10–200 ms) eliciting Ca^{2+} influx. The results showed that the *Klhl18*^{lowf} mutation did not affect the Ca^{2+}-triggered IHC exocytosis measured upon depolarization pulses of 10–50 ms, while sustained IHC exocytosis measured upon longer depolarization pulses (200 ms) was significantly decreased in homozygous mutants compared to WT controls (Fig. 1m–o). It is plausible that Klhl18 is involved in the recycling of synaptic vesicles, which relies on functional cytoskeleton structures, and that the lack of normal Klhl18 slows the recycling of synaptic vesicles and therefore reduces sustained IHC exocytosis as measured upon longer stimulation. The dual-AAV system restored the sustained IHC exocytosis after 200 ms depolarization pulses in homozygous mutants (Fig. 1m–o), which confirms that the *Klhl18*^{lowf} mutation was corrected in IHCs via CRISPR/Cas9-mediated HMEJ. However, in this study we found no significant difference in voltage-gated Ca^{2+}-current (I_{Ca}) among dual-AAV-treated homozygous *Klhl18*^{lowf}, untreated homozygous *Klhl18*^{lowf}, and WT IHCs (Supplementary information, Fig. S14), which indicates that the *Klhl18*^{lowf} mutation did not influence the I_{Ca} of IHCs.

We also used ELISA to test the immune response to AAV vectors at 28 days after injection and found no significant difference in the immune response between the injected and non-injected mice (Supplementary information, Fig. S15).

In conclusion, our HMEJ-based system provides a great advance in applying the HDR strategy for gene editing in mammalian cochlear hair cells. However, to obtain better therapeutic effect, there is still an urgent need for developing new strategies to further augment the knock-in efficiencies in nondividing mammalian cells. Still, the proof-of-concept results provided here show promise for further development of HMEJ-based strategies for the repair of point mutations that cause inherited hearing loss as well as other human genetic diseases.

Xi Gu[1,2,3,4,9], Xinde Hu[5,9], Daqi Wang[1,2,4,9], Zhijiao Xu[1,2,4], Fang Wang[1,2,4], Di Li[6,7], Geng-lin Li[1,2,4], Hui Yang[5], Huawei Li[1,2,4,8]✉, Erwei Zuo[7]✉ and Yilai Shu[1,2,4]✉

[1]ENT institute and Department of Otorhinolaryngology, Eye & ENT Hospital, State Key Laboratory of Medical Neurobiology and MOE Frontiers Center for Brain Science, Fudan University, Shanghai, China. [2]Institutes of Biomedical Sciences, Fudan University, Shanghai, China. [3]Department of Otolaryngology, the First Affiliated Hospital of Fujian Medical University, Fuzhou, China. [4]NHC Key Laboratory of Hearing Medicine (Fudan University), Shanghai, China. [5]Institute of Neuroscience, State Key Laboratory of Neuroscience, Key Laboratory of Primate Neurobiology, CAS Center for Excellence in Brain Science and Intelligence Technology, Shanghai Research Center for Brain Science and Brain-Inspired Intelligence, Shanghai Institutes for Biological Sciences, Chinese Academy of Sciences, Shanghai, China. [6]State Key Lab for Conservation and Utilization of Subtropical Agric-Biological Resources, Guangxi University, Nanning, China. [7]Shenzhen Branch, Guangdong Laboratory for Lingnan Modern Agriculture, Genome Analysis Laboratory of the Ministry of Agriculture, Agricultural Genomics Institute at Shenzhen, Chinese Academy of Agricultural Sciences, Shenzhen, China. [8]The Institutes of Brain Science and the Collaborative Innovation Center for Brain Science, Fudan University, Shanghai, China. [9]These authors contributed equally: Xi Gu, Xinde Hu, Daqi Wang. ✉email: hwli@shmu.edu.cn; erweizuo@163.com; yilai_shu@fudan.edu.cn

REFERENCES

1. Carpena, N. T. & Lee, M. Y. *Genomics Inform.* **16**, e20 (2018).
2. Cox, D. B., Platt, R. J. & Zhang, F. *Nat. Med.* **21**, 121–131 (2015).
3. Yang, Y. et al. *Nat. Biotechnol.* **34**, 334–338 (2016).
4. Mianne, J. et al. *Genome Med.* **8**, 16 (2016).
5. Yao, X. et al. *Cell Res.* **27**, 801–814 (2017).
6. Ingham, N. J. et al. *PLoS One* **16**, e0258158 (2021).
7. Paquet, D. et al. *Nature* **533**, 125–129 (2016).
8. Hu, X. et al. *Cell Discov.* **5**, 49 (2019).
9. Gao, X. et al. *Nature* **553**, 217–221 (2018).
10. Adams, J., Kelso, R. & Cooley, L. *Trends Cell Biol.* **10**, 17–24 (2000).

ACKNOWLEDGEMENTS

We thank Professor Karen P Steel and Dr. Neil J Ingham (Wolfson Centre for Age-Related Diseases, King's College London) for providing the *Klhl18*^{lowf} mutant mice and for discussion of the findings. This work was supported by grants from the National Key R&D Program of China (2020YFA0908201, 2017YFA0103900), the National Natural Science Foundation of China (82171148, 81822011, 31922048, 81830029, 82171141, 82000992), the Science and Technology Commission of Shanghai Municipality (21S11905100, 21JC401000), Clinic Research Plan of SHDC (SHDC2020CR4083), "Shuguang Program"supported by Shanghai Education Development Foundation and Shanghai Municipal Education Commission (20SG08), and the Agricultural Science and Technology Innovation Program (to E.Z.).

AUTHOR CONTRIBUTIONS

X.G., X.H., and D.W. designed the research, performed in vitro and in vivo experiments, analyzed the data, generated the figures, and wrote the manuscript. X.H. and D.W. constructed the HMEJ-based system and measured the editing efficiencies in vitro and in vivo. X.G. performed in vivo injection, in vitro culture, immunofluorescence staining, confocal microscopy observation, SEM sample preparation and observation, and ABR and DPOAE measurements. Z.X. analyzed the hearing data and helped write the manuscript. H.Y. and D.L. assisted with genome editing and helped with the sequencing data analysis. G.L. and F.W. performed the whole-cell patch-clamp electrophysiological recording and helped write the manuscript. Y.S., E.Z., and H.L. conceived the project, designed and supervised the research, and wrote the manuscript. All authors reviewed, edited, and approved the manuscript.

COMPETING INTERESTS

The authors declare no competing interests.

ADDITIONAL INFORMATION

Supplementary information The online version contains supplementary material available at https://doi.org/10.1038/s41422-022-00624-y.

Correspondence and requests for materials should be addressed to Huawei Li, Erwei Zuo or Yilai Shu.

Reprints and permission information is available at http://www.nature.com/reprints